Journal of Structural Geology, Vol. 9, No. 7, pp. 835 to 844, 1987
Printed in Great Britain

0191–8141/87 $03.00 + 0.00

Hinge migration as a mechanism of superimposed folding

F. ODONNE

Laboratoire de Radiogéologie et de Mécanique des Roches, Université de Bordeaux I, Avenue des Facultés, 33405 Talence Cédex, France

and

P. VIALON

Institut de Recherches Interdisciplinaires de Géologie et de Mécanique, Université de Grenoble I, B.P. n° 68, 38402 Saint Martin d'Hères Cédex, France

(*Received* 3 *April* 1986; *accepted in revised form* 30 *December* 1986)

Abstract—Paraffin wax analogue modelling of superimposed folding shows how early fold shape and orientation determine fold-axis orientation, type of interference pattern and mechanism of superposed folding. During two successive deformations, the behaviour depends on the angle between the first and second compression directions. (i) When they are perpendicular to each other, classic superposed folding with either domes and basins, or folds with vertical axes develop, depending on whether the earlier folds were open or closed. (ii) When the two compression directions are oblique, the earlier folds rotate. The degree of rotation depends on the angle between the first folds and the later compression direction and is proportional to the amount of strain. The orientations of the new folds are close to those of the earlier open folds. The final deformation pattern consists of domains where the orientations of the axes depend on whether the early folds were previously either open or closed. Many early folds are reused to become later folds by the mechanism of hinge migration.

These results are consistent with the pattern of superimposed folding observed in the Devoluy structure of the French Alps. They show that simply by studying the directions of fold axes in areas of superposed folding, it is not possible to define compression directions. Moreover there is the possibility that superposed folding may go unnoticed if hinge migration has occurred.

INTRODUCTION

WHEN A folded structure is submitted to a second compression, the reaction of early folds with subvertical axial surfaces could be of two types: superimposed folds may appear, the geometries of which are well established (Ramsay 1967, p. 520, Thiessen & Means 1980); or early folds may be reused (Tobisch 1967), becoming new folds as a result of hinge migration. The purpose of this study was to determine how the orientation and shape of early folds decide which of these two reactions occur.

We have chosen two examples to illustrate this research. Firstly an example in the field: the Devoluy limestone massif in the southern French Alps, which presents two successive foldings (Lemoine 1972). For the most part we find two main sets of folds, the first set trending E–W and the second superimposed set trending N–S. In some places, however, only one set of folds appears, which trends more or less midway between N–S and E–W. We must now compare these differences in geometry with the positions and forms of the early folds and with the directions of successive compressions. The second example is an analogue model consisting of seven paraffin wax sheets which are subjected to two successive compressions. The directions along which these compressions act vary from one experiment to another. Each fold that forms is labelled throughout the experiment and its evolution can be observed in relation to the direction of successive compressions. An exact analogy between the field studies and the model is difficult to achieve, Nature being infinitely more complex than a model, which is necessarily only schematic. However, if results show that there is a degree of agreement between the two examples, this would suggest that similar deformation histories may be involved. The conclusions drawn would thus be valid not only in an experimental situation, but could also be applied to the development of geological structures in the field.

MULTIPLE FOLDING IN THE DEVOLUY MASSIF

In the sedimentary cover of the southern French Alps there are many examples of superimposed folding (Lemoine 1972). In the Devoluy Massif (Fig. 1) the two phases of folding are clearly dated (Glangeaud & Albissin 1958, Goguel 1963, Gidon *et al.* 1970, Arnaud 1974). The first phase, linked to early Alpine events (Caby 1973), is Turonian (88–95 Ma) (Mercier 1958). The corresponding folds (F_1), usually inclined, trend NE–SW or E–W, perpendicularly to the classical French Alpine orientation. The second folds (F_2), linked to middle Alpine events, were formed at the end of the Oligocene (Lemoine 1972) and their orientation is generally N–S. The great Devoluy Syncline (F_2), with a trend of 170°, affects Senonian (latest Cretaceous) limestones and the Palaeogene (Fig. 2). Around the edges of the massif, F_1 folds that have undergone the two succes-

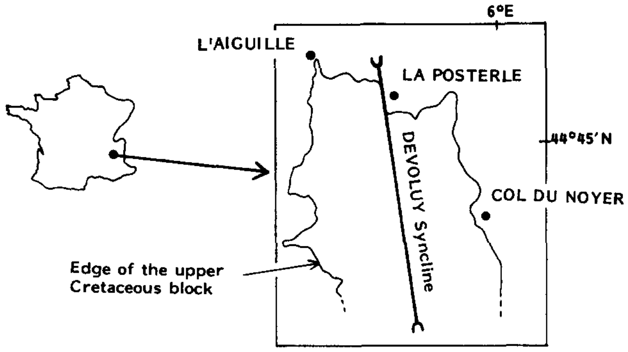

Fig. 1. Geographical location of the Devoluy Massif in the southern French Alps. Areas shown here are situated at the edge of the Upper Cretaceous block.

sive phases of compression are exposed. A vertical section (perpendicular to the axis of the Devoluy Syncline) from the St Bonnet 1/50,000 geological map, shows that deformation due to the second compression phase produced a shortening of about 30% along the E–W direction. This estimate does not take into consideration the thickening that may have occurred in the layers before and during folding (Cobbold 1975, Gairola & Kern 1984).

Our studies have concentrated on the reaction of the early folds (F_1) to the second compression. Superimposed folds may appear, or F_1 folds may be reused during F_2 folding, becoming F_2 folds as a result of hinge migration. Let us examine the features of these alternatives.

Superimposed folding

At the Col du Noyer (Fig. 1) Upper Jurassic formations form a fold trending 070°, inclined towards the north and emphasized by second-order folds on the inverted limb. On a kilometric scale this fold is refolded into a type 2 interference pattern (Ramsay 1967, p. 525) by the Devoluy Syncline. The western part of the fold hinge plunges steeply W (60°) under the Senonian block. Further east the intersection of cleavage and bedding (in marly limestone of the Upper Oxfordian) suggests a subhorizontal hinge. On a decametric scale, F_2 folds formed after the cleavage had appeared on the limbs of

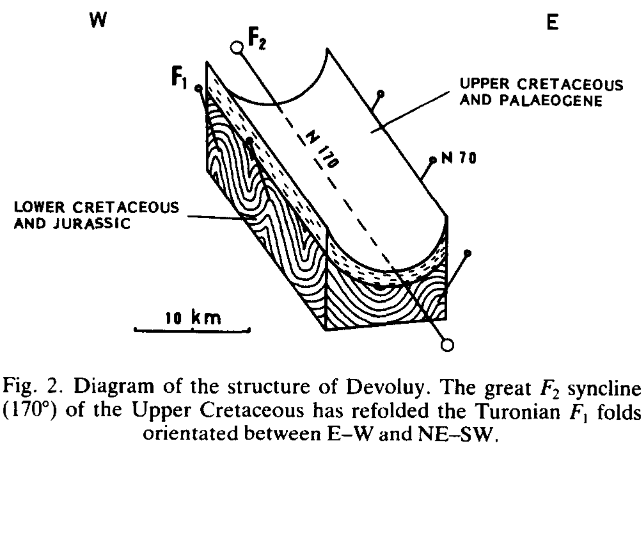

Fig. 2. Diagram of the structure of Devoluy. The great F_2 syncline (170°) of the Upper Cretaceous has refolded the Turonian F_1 folds orientated between E–W and NE–SW.

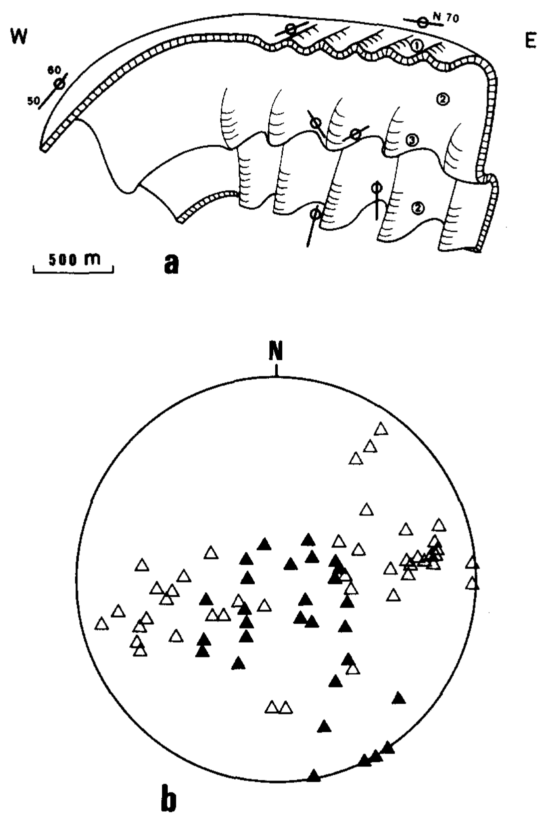

Fig. 3. (a) Col du Noyer. Diagram showing large F_1 fold which trends 070°. The F_2 fold has refolded the axis of the earlier fold of which the plunge varies from E to W. On the limbs, F_2 folding is present in the form of small folds that are horizontal in the normal limb (location 1), subvertical in the overturned limb (location 2), and superimposed over the second-order F_1 folds in the overturned limb where domes and basins appear (location 3). (b) Axes of the Col du Noyer folds, F_1 folds (white triangles) and F_2 folds (black triangles) on a Wulff net (lower hemisphere).

the major fold. On the normal limb these F_2 folds trend 160° (Fig. 3a, location 1). On the overturned limb they are subvertical (Fig. 3a, location 2) and in some places with second-order F_1 folds they create a type 1 interference pattern (Ramsay 1967) with the classic geometry of domes and basins (Fig. 3a, location 3); the orientations of the F_1 folds are therefore very dispersed (Fig. 3b).

Hinge migration

Near La Posterle (Fig. 1) the folds affect Upper Jurassic limestones. They trend for the most part between 030 and 050°. One fold presents cracks (tension fissures on the outer arc of the layers) which run parallel to its axial direction (023°). These longitudinal veins (Droxler & Schaer 1979) cut across older cracks lying obliquely across the present hinge (Figs. 4a and 10a). These oblique cracks trend from 023 to 050° and, like the longitudinal veins, they are abundant in the hinge zone. Near l'Aiguille (Fig. 1), in Upper Jurassic limestone formations, one fold with an axial direction of 028° can be clearly distinguished from the rest, which trend 046 to 053°. All these folds show a marked degree of fracturing (140°) perpendicular to the axial direction (Fig. 5a). On the 028°-trending fold, and on this one only, fracturing runs obliquely across the axial direction and is dispersed

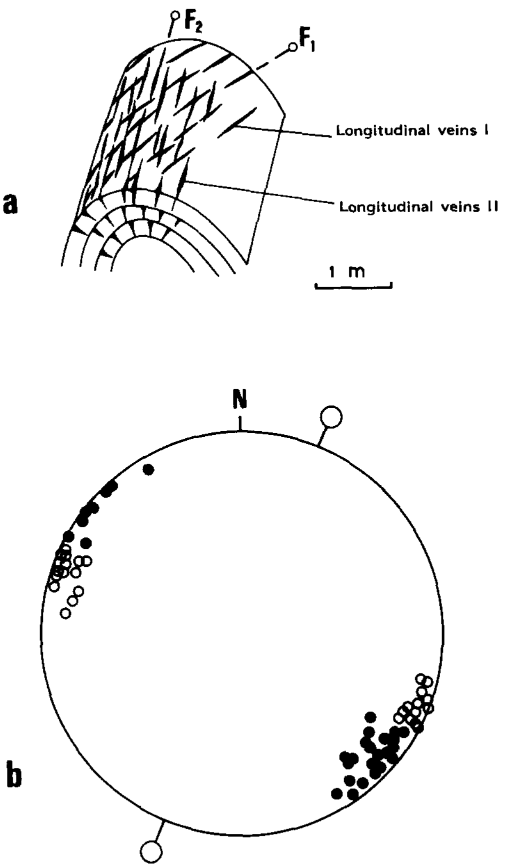

Fig. 4. (a) La Posterle. Diagram of the 023°-trending fold with longitudinal veins II parallel to the axis F_2, and refolding of the longitudinal veins I oriented 050°. These cracks are evidence that an early fold F_1 (050°) has been reactivated during the F_2 folding. (b) Poles to longitudinal veins I (black circles) continually changing to become longitudinal veins II (white circles). Unfolded stratification on a stereographic net (lower hemisphere).

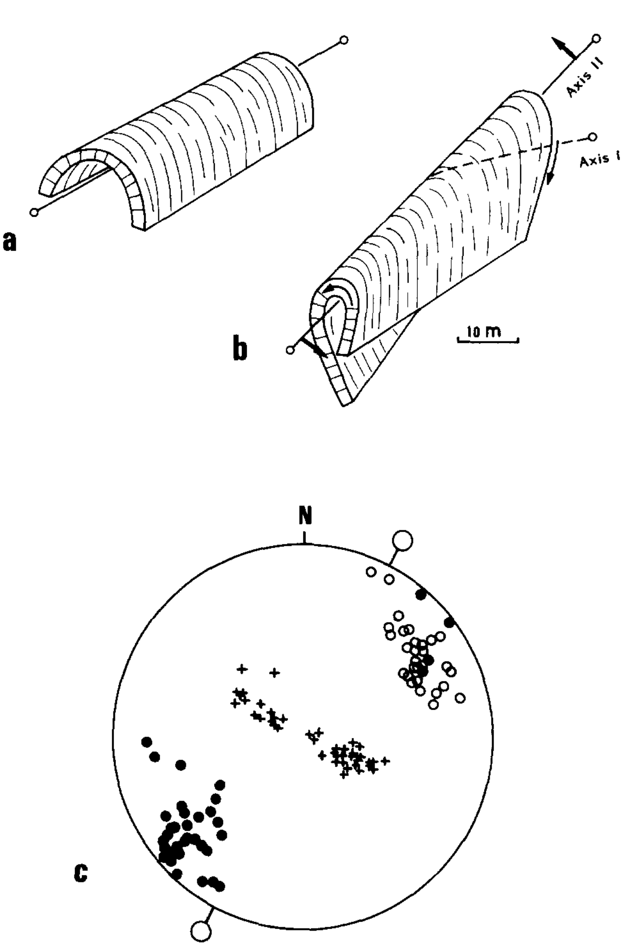

Fig. 5. (a) L'Aiguille. Diagram of an F_1 fold trending 050° with fracturing across the axis. (b) The F_2 fold trending 028° has refolded the fractures and its hinge has migrated to its present position. (c) Fractures across the axis of the fold have been swung round onto the limbs of the fold trending 028°, NW limb (black circles) and SE limb (white circles). The crosses represent poles of bedding (Wulff net, lower hemisphere).

over the limbs (Fig. 5b). These two early folds seem to have rotated to become F_2 folds by hinge migration.

The 023°-trending fold of La Posterle presents early longitudinal veins parallel to the hinge of the fold in its F_1 position. This fold was rotated from 050 to 023° and throughout this rotation, longitudinal veins were continually appearing at every stage (Fig. 4b). The last crack to appear is parallel to the present axial direction (F_2 fold 023°). The 028°-trending fold of l'Aiguille appears to be a previously 050°-trending fold that was re-oriented (Fig. 5c). The attitudes of perpendicular fractures demonstrate re-orientation: they have been tilted in opposite directions on each limb of the fold. This mechanism of hinge migration has already been described in different contexts as part of a progressive deformation (Wegmann 1932, Hudleston 1973, Cobbold 1975, Borradaile 1978, Brun 1978, Gray 1981) but never (except Tobisch 1967), as is the case here, in the context of superimposed folding.

ANALOGUE MODELS

The models devised for our experiment consist of seven sheets of paraffin wax (MERCK paraffin wax; melting point: 46–48°C; thickness of each layer: 1.5 mm) separated by silicone grease (RHONE-POULENC, S-428). The experiment was carried out in a thermostatically controlled airtight container maintained at 30°C. At this temperature the viscosities of the materials are 3×10^5 Pa.s for the paraffin wax and 5×10^2 for the grease (Odonne & Vialon 1983). This represents a viscosity contrast of 600:1, and according to Dixon & Summers (1985), this figure corresponds to that suggested by Biot (1961) for the contrast between limestone and clay; it also respects the rules of similarity laid down by Hubbert (1937). The choice of viscous materials to represent deformation in limestones in an upper structural level is in accordance with observations made on the scale of a massif (Laubscher 1975) and of a sample (Gratier 1984).

Deformation of the models took place in rectangular boxes made of plexiglass; one of the short sides of each box is moveable (Fig. 6). Compression creates buckling folds (Ramberg 1963) which are of decreasing size the further they are from the moving side of the box. In order to limit this softening of folds, the base of the model rests on a layer of grease, the viscosity of which is

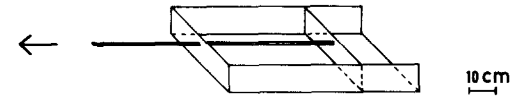

Fig. 6. Principle of the plexiglass boxes. One side moves to compress the model.

reduced to 10 Pa.s by the addition of silicone oil. There are two stages to each experiment.

Stage 1: a multilayer model undergoes compressive deformation. Its width remains unchanged (60 cm) but its length is reduced from 70 to 53 cm; the extension can be expressed as $e = -0.24$. The crests of the folds on the surface of the model are marked with blue ink; they are '*F*' folds.

Stage 2: from each folded model a smaller model is cut, which is compressed again in a small plexiglass box (Fig. 7). The length of the model is reduced from 40 to 28 cm; hence $e = -0.3$. After this second deformation, two sets of folds may co-exist on each model: (i) the early fold (*F* folds of stage 1) which have undergone the second deformation and have now become 'F_1' folds (after rotation and reactivation); the ink marks are preserved and demonstrate the previous positions and lengths which are not exactly those of *F*; (ii) the second set of folds consists of new folds which appear during the second deformation; they are 'F_2' folds, marked with red ink. Stage 2 corresponds to what is observed in the Devoluy Massif with F_1 and F_2 folds.

The angle between the directions of the two compressive deformations (angle $Z_1 \wedge Z_2$) may vary from 0 to 90°. Here we present the results of six experiments where the value of $Z_1 \wedge Z_2$ was 15, 30, 45, 60, 75 and 90° (Fig. 8). Some of the experiments were carried out a second time to ensure that the results could be reproduced.

For convenience we shall assume that the Z_2 compression always acts from east to west, which should thus create F_2 folds that trend N–S. Then the *F* folds on each model have an orientation equal to the value of the angle $Z_1 \wedge Z_2$ (i.e. *F* folds from the 30° model trend 030°) and the gradual decrease in folding is towards the NW. We will first consider each set of folds, *F*–F_1 folds then F_2 folds; then we will examine how superimposed folding and hinge migration appear.

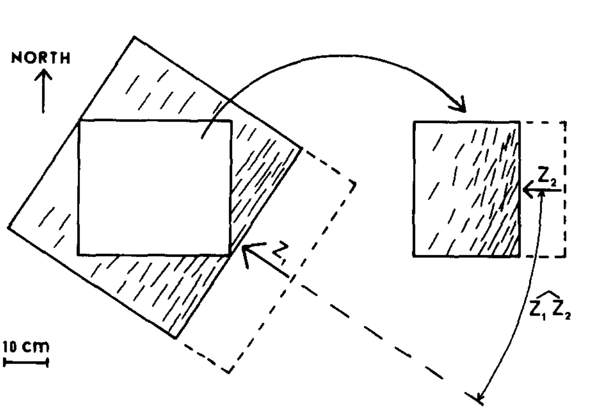

Fig. 7. The multilayer model of paraffin wax and grease has been folded once under the effect of a compression Z_1. A smaller model is cut from it which undergoes a second compression Z_2. The angle between the two directions of compression ($Z_1 \wedge Z_2$) is known. The direction of the folds is given in relation to 'North' which lies perpendicular to the direction of Z_2.

F–F_1 *folds*

F folds become F_1 folds during the second compressive deformation. The arithmetic means of the orientations change and get closer to N–S by rotation in an anticlockwise direction (except in the case of the 90° model). The *F* folds were perpendicular to the direction of the first compression; the F_1 folds are no longer so. Maximum fold rotation is observed in the 45 and 60° models where it reaches about 10°. The rotation of the folds agrees with J. G. Ramsay's computations (1967, p. 131) on the changes in angle during deformation. However, from *F* folds to F_1 folds the orientations of the folds disperse (standard deviations increase) especially in the 75 and 90° models (Fig. 11). It is thus now impossible to deduce directly from the orientation of the F_1 folds the direction of the first compression, if the intensity of the second deformation is not known.

F_2 *folds*

According to the convention adopted earlier, the second compression runs from E to W and should form F_2 folds which trend N–S. Figure 9, however, shows that the F_2 folds are close to N–S only in the 90° case, and on the other models the deviation may reach 20°. It would appear that F_2 folds have a tendency to align with F_1 folds, and this parallelism is practically total for the 15 and 30° models, as Ghosh & Ramberg have shown (1968). In fact, when angle $Z_1 \wedge Z_2 = 45°$ and below (Figs. 8 and 9) it is very difficult to distinguish two successive phases of folding simply by examining the axial directions of the folds. Thus the F_1 folds are not simply markers, they provide linear reinforcement for the model (Cobbold & Watkinson 1981) and cause the second shortening phase to be perpendicular to the F_1 folds but not perpendicular to the direction of the second compression.

Superimposed folding

Where the value of $Z_1 \wedge Z_2$ is high, superimposed folding is observed (Ghosh & Ramberg 1968, Skjernaa 1975) in areas of the models where F_1 folds are open folds (inter-limb angle >70°, in Fleuty 1964). Classic features are presented, with domes and basins. Where F_1 folds are close folds (inter-limb angle <70°) F_2 folds appear with subvertical axial directions, because the limbs of the folds are subvertical. The axial surfaces of the F_1 folds are themselves folded (Watkinson 1981). This accounts for the fact that the axial directions of the F_1 folds on the 75 and 90° models (Fig. 11) are highly dispersed.

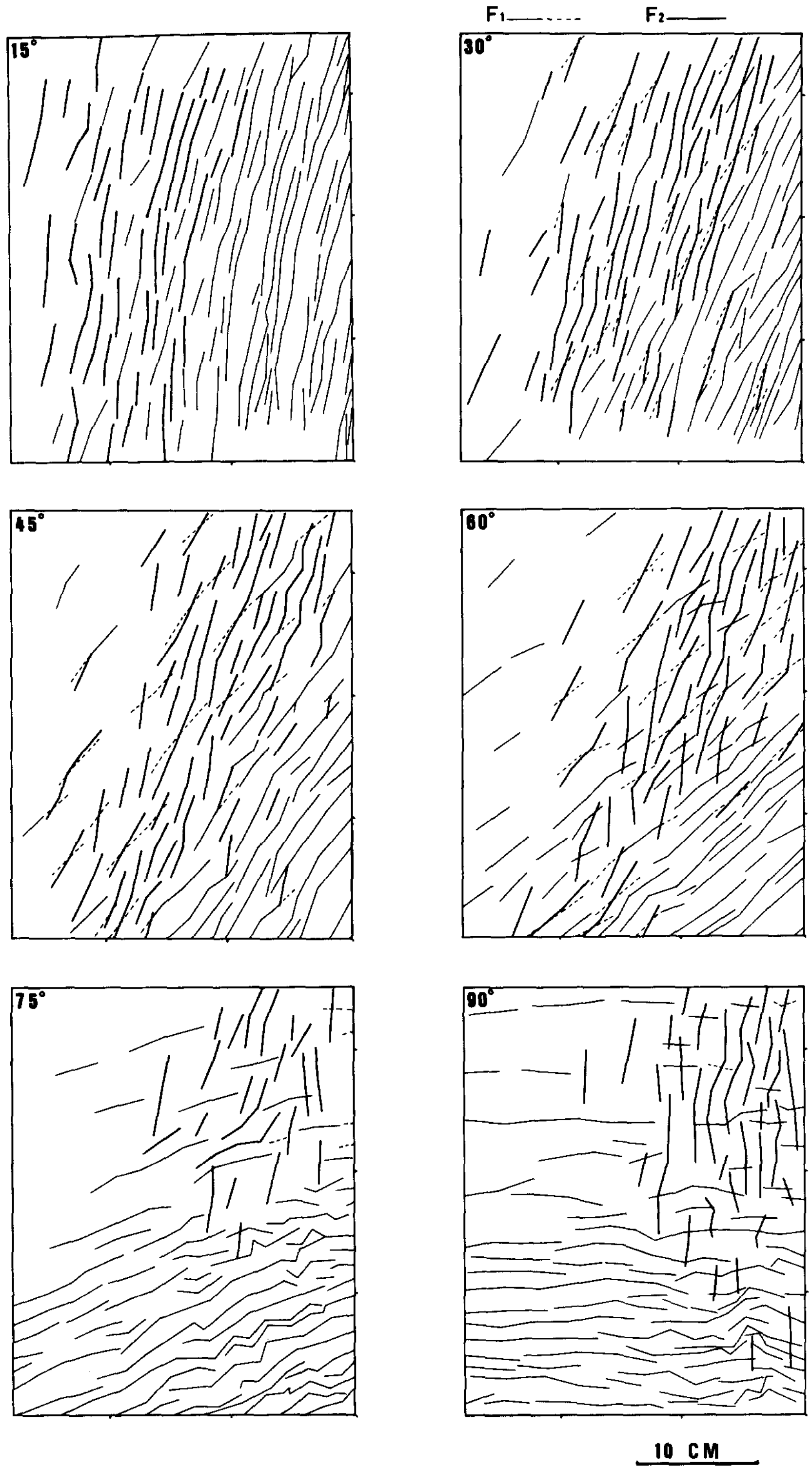

Fig. 8. On the folded surface of each model (angle $Z_1 \wedge Z_2$ = 15, 30, . . . , 90°) can be seen F_2 folds (thick lines), F_1 folds (fine lines), and F_1 folds that have been effaced or have become F_2 folds by hinge migration (fine dotted lines). The direction of Z_2 is always E–W.

Hinge migration

Where the value of $Z_1 \wedge Z_2$ is low (30°, 45°) there are none of the classic features of superimposed folding. The F_2 folds appear in one of two ways: (i) they either appear with an orientation close to that of the F_1 folds, which may themselves continue to develop (Goguel 1965); or (ii) *F* folds are transformed directly into F_2 folds. In this case it is no longer simply a question of clockwise rotation by the *F* folds which then become F_1 folds, but a hinge migration. The blue lines on the crests of the *F* folds are now oblique to the new folds (F_2), in exactly the same way as early cracks on the 023°-trending fold at La Posterle (see Figs. 4a, 10a & b). Hinge migration is thus a mechanism of superimposed folding. Only open folds may be reused in this way. If the folds are too close they are not able to develop any further (Cobbold 1976). This confirms the idea already ex-

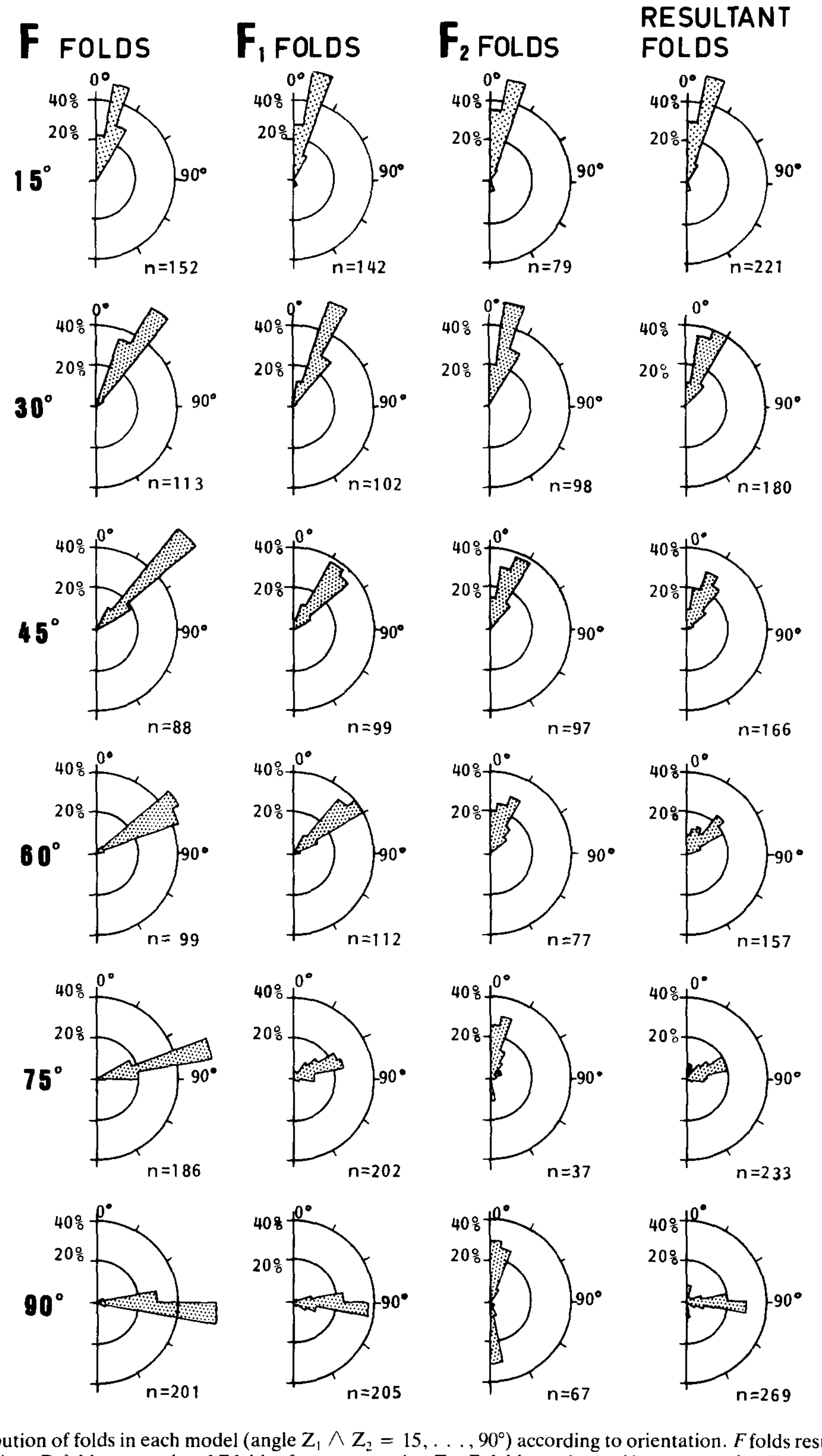

Fig. 9. Distribution of folds in each model (angle $Z_1 \wedge Z_2$ = 15, . . . , 90°) according to orientation. *F* folds result from the first compression, F_1 folds are tracks of *F* folds after compression Z_2, F_2 folds are formed by compression Z_2, resultant folds are all folds observed after the total deformation. *n* = number of fold segments.

pressed, that each model is divided into two main areas: one with open *F* folds and another with closed *F* folds. According to Hobbs *et al.* (1976, p. 353) and Williams (1985), the occurrence of hinge migration reinforces the idea that the orientation of folds may not be used directly for the correlation of structures in multiply deformed terrains.

The 60° model is midway between these two extremes (models with a small angle $Z_1 \wedge Z_2$ and those with a large angle $Z_1 \wedge Z_2$). Some classic features of superimposed folding are present at the same time as hinge migration (Fig. 8). The transition from one type of folding to another does not seem to be sudden. There is instead a progressive changeover from one type to another as the value of angle $Z_1 \wedge Z_2$ changes.

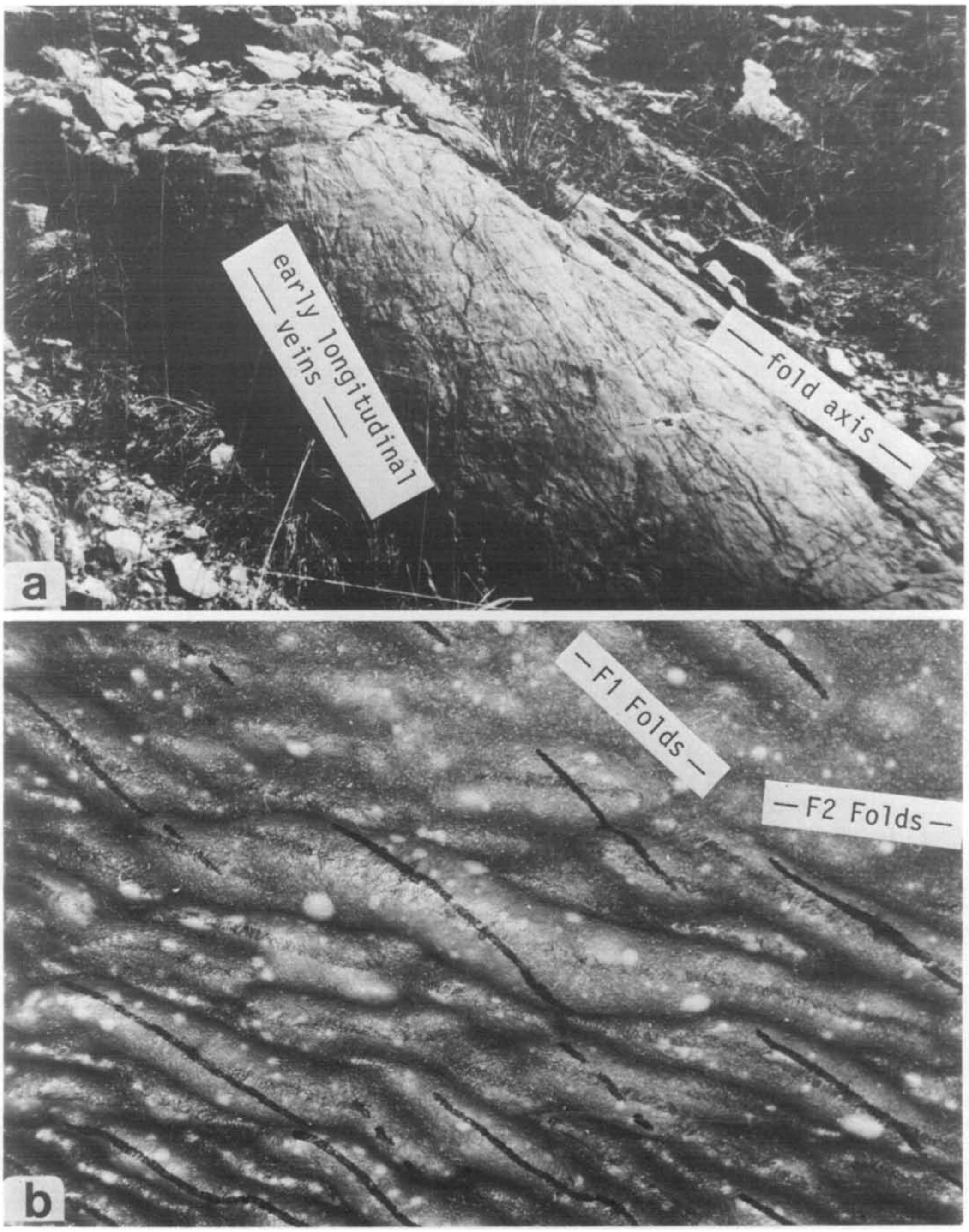

Fig. 10. (a) In the Devoluy, at La Posterle, a fold presents longitudinal veins oblique to its axis. They are evidence of the migration of the early hinge to accommodate the fold to the new compression. (b) Detail of the 45° model. In the centre of the photograph, an F fold (045°), marked with dark ink, has become an F_2 fold (020°) by means of hinge migration. The F folds whose hinges have not migrated have become F_1 folds (037°) after anticlockwise rotation. 'North' in this model is to the right of the photograph.

COMPARISON OF ANALOGUE MODEL AND FIELD WORK

The Devoluy Massif and the corresponding model present many similar points: the same rheological behaviour; two compressive deformations, one obviously occurring after the other; equal intensity of deformation as a result of the second compression (e = −0.3). We have already analysed separately the natural and the experimental folding. Now let us try to see points of comparison between the findings relating to superimposed folding and hinge migration. In this way we shall be able to show how the model has contributed to our understanding of the Devoluy folds.

At the Col du Noyer superimposed folding has given rise to subvertical F_2 folds on the limbs of an 070°-trending fold. The direction of the second compression is about 080° and is presumed to be perpendicular to the great 170°-trending syncline of Senonian limestone. The model that most closely resembles this situation is the 75° model (Figs. 3a and 8). At La Posterle and l'Aiguille F_1 folds (050°) become F_2 folds (025°) with hinge migration. The geometry of this situation seems to be the same as that of the 60° model, where the mean directions of the F_1 and F_2 folds are 50.8 and 21.5°, respectively (Fig. 11). However, the folds which undergo hinge migration are F folds not F_1 folds. The 10° anticlockwise rotation which turned the F folds into an F_1 has not been taken into consideration and it must be assumed that the orientation of the early folds was 060°. The early folds in the field trend 070 or 060°; this 10° dispersion agrees with the values of standard deviation of F folds in the models (Fig. 11). Superimposed structures in the Devoluy formation correspond best to the 75 and 60° models (see Figs. 3, 4 and 8); thus the direction of the first Devoluy compression would trend 160°, perpendicular to the early folds.

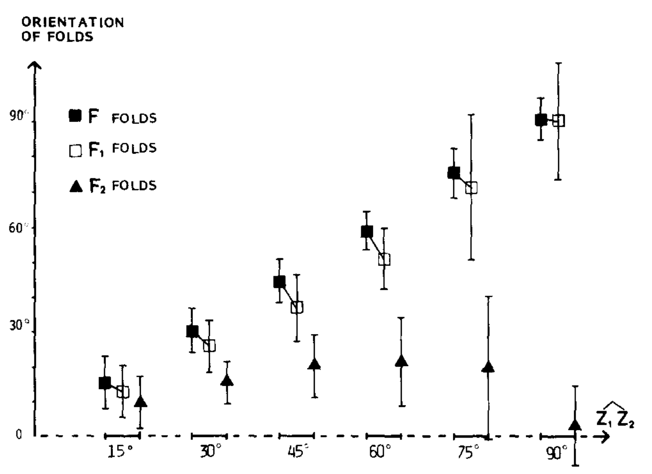

Fig. 11. Mean values of the orientation of the different sets of folds for each model (angle $Z_1 \wedge Z_2$ = 15, . . . , 90°): F, which result from the first compression; F_1 and F_2, which result from the second compression. The interval shown on either side of each mean represents standard deviation.

CONCLUSION

In a previously folded structure the direction of a second compression is not sufficient to explain the orientation of new buckle folds. The geometry of the early folds and their orientation and shape have a bearing on the second compression phase and affect the results. This is supported by field studies (Devoluy Massif) and analogue modelling using paraffin wax. Both field work and experiments show the following points quite clearly.

(i) If the angle made by the two compression directions is large (60–90°), superimposed folding is produced, the type of folding dependent on whether the early folds were open or closed. If the early folds were open, then domes and basins are produced by the second compression; if they were closed then subvertical superimposed folds will appear on the limbs.

(ii) If the angle between the two compression directions is small (<60°) classic superimposition does not appear and the axial directions of the early folds (F_1) and the later folds (F_2) are closer together. Some open F folds may become F_2 folds directly when a hinge from the first stage migrates and is replaced by another which then becomes part of the set of F_2 folds. In the field, migration of longitudinal veins on the outer arc of a fold or the dispersion of fractures on the limbs of folds may show where this has occurred.

Thus, the total deformation pattern appears to consist of two types of juxtaposed areas. In the first type of area the early folds were open, in the second type they were closed. Each area delimits a domain in which deformation is almost homogeneous and has its own main direction. Deformation of the structure as a whole is then the resultant of the deformations of these areas.

Finally, the angle between the two main sets of folds will seldom be equal to, though it is often smaller than, the angle made by the two compression directions. This is because after the second compression, the early folds no longer have the early orientation, and the rotation they undergo is a function of their orientation and of the intensity of the second compressive deformation. At the same time, the F_2 folds are not perpendicular to the second compression direction. The early structure therefore presents a linear anisotropy, where later folds copy exactly the early folds in a mimetic process and the later folds reuse the early folds with clearly evident hinge migration. This convergence of the axial directions of folds may be so considerable that only one fold direction is observed. This, however, is not proof that all the folds were formed at the same time. The presence or absence of hinge migration may then indicate if folding was or was not superimposed.

Acknowledgements—The authors are very grateful to the Société Nationale Elf Aquitaine (Production) who have largely financed this research programme and have permitted publication, and in particular to Mr P. Janot who instigated the work. They would also like to thank Professor M. Gidon who very kindly gave us the benefit of his wide knowledge of the Devoluy Massif, and the Centre d'Hydrogéologie of the University of Bordeaux I for generously giving us both technical and secretarial assistance.

REFERENCES

Arnaud, H. 1974. Nouvelles données sur la tectonique "anté-sénonienne" des environs de La Jarjatte (Devoluy occidental). *C.r. Acad. Sci., Paris Sér.* **D 278**, 697–700.

Biot, M. A. 1961. Theory of folding of stratified viscoelastic media and its implications in tectonics and orogenesis. *Bull. geol. Soc. Am.* **72**, 1595–1620.

Borradaile, G. J. 1978. Transected folds: a study illustrated with examples from Canada and Scotland. *Bull. geol. Soc. Am.* **89**, 481–493.

Brun, J. P. 1978. L'enroulement des charnières de plis pendant la déformation progressive: arguments microtectoniques. *VIe Reunion Annuelle des Sciences de la Terre. Orsay (France).*

Caby, R. 1973. Les plis transversaux dans les Alpes occidentales: implications pour la genèse de la chaîne alpine. *Bull. Soc. geol. Fr.*, 7 *Ser.* **XV**, 624–634.

Cobbold, P. R. 1975. Fold propagation in single embedded layers. *Tectonophysics* **27**, 333–351.

Cobbold, P. R. 1976. Mechanical effects of anisotropy during large finite deformations. *Bull. Soc. geol. Fr.*, 7 *Ser.* **XVIII**, 1497–1510.

Cobbold, P. R. & Watkinson, A. J. 1981. Bending anisotropy: a mechanical constraint on the orientation of fold axes in an anisotropic medium. *Tectonophysics* **72**, T1–T10.

Dixon, J. M. & Summers, J. M. 1985. Recent development in centrifuge modelling of tectonic processes: equipment, model construction techniques and rheology of model material. *J. Struct. Geol.* **7**, 83–102.

Droxler, A. & Schaer, J. P. 1979. Déformation cataclastique plastique lors du plissement, sous faible couverture, de strates calcaires. *Eclog. geol. Helv.* **72**, 551–570.

Fleuty, M. J. 1964. The description of folds. *Proc. Geol. Ass.* **75**, 461–492.

Gairola, V. K. & Kern, H. 1984. Microstructure and texture in experimentally folded single-layer rock salt. *J. Struct. Geol.* **6**, 201–213.

Ghosh, S. K. & Ramberg, H. 1968. Buckling experiments on intersecting fold patterns. *Tectonophysics* **5**, 89–105.

Gidon, M., Pairis, J. L., Arnaud, H., Aprahamian, J. & Uselle, J. P. 1970. Les déformations tectoniques superposées du Devoluy méridional. *Géol. Alpine.* **46**, 87–110.

Glangeaud, L. & d'Albissin, M. 1958. Les phases tectoniques du N.E. du Devoluy et leur influence structurologique. *Bull. Soc. geol. Fr.*, 6 *Ser.* **VIII**, 675–688.

Goguel, J. 1963. L'interprétation de l'arc des Alpes occidentales. *Bull. Soc. geol. Fr.*, 7 *Ser*, 20–33.

Goguel, J. 1965. *Traité de Tectonique.* Masson, Paris.

Gratier, J. P. 1984. La déformation des roches par dissolution-cristallisation. Unpublished thèse d'Etat, Grenoble University.

Gray, D. R. 1981. Cleavage–fold relationships and their implications for transected folds: an example from southwest Virginia, U.S.A. *J. Struct. Geol.* **3**, 265–277.

Hobbs, B. E., Means, W. D. & Williams, P. F. 1976. *An Outline of Structural Geology.* Wiley, New York.

Hubbert, K. 1937. Theory of scale models as applied to the study of geologic structures. *Bull. geol. Soc. Am.* **48**, 1459–1520.

Hudleston, P. J. 1973. Fold morphology and some geometrical implications of theories of fold development. *Tectonophysics* **16**, 1–46.

Laubscher, H. P. 1975. Viscous components in Jura folding. *Tectonophysics* **27**, 239–254.

Lemoine, M. 1972. Rythme et modalités des plissements superposés dans les chaînes subalpines méridionales des Alpes occidentales françaises. *Geol. Rdsch.* **61**, 975–1010.

Mercier, J. 1958. Sur l'âge de la phase turonienne à l'Ouest du massif du Devoluy. *Bull. Soc. geol. Fr.*, 6 *Ser.* **VII**, 689–697.

Odonne, F. & Vialon, P. 1983. Analogue models of folds above a wrench fault. *Tectonophysics* **99**, 31–46.

Ramberg, H. 1963. Strain distribution and geometry of folds. *Bull. geol. Instn. Univ. Uppsala* XLII **4**, 20.

Ramsay, J. G. 1967. *Folding and Fracturing of Rocks.* McGraw-Hill, New York.

Skjernaa, L. 1975. Experiments on superimposed buckle folding. *Tectonophysics* **27**, 255–270.

Thiessen, R. L. & Means, W. D. 1980. Classification of fold interference patterns: a re-examination. *J. Struct. Geol.* **2**, 311–316.

Tobisch, O. T. 1967. The influence of early structures on the orientation of late-phase folds in an area of repeated deformation. *J. Geol.* **75**, 554–564.

Watkinson, A. J. 1981. Patterns of fold interference: influence of early fold shapes. *J. Struct. Geol.* **3**, 19–23.

Wegmann, C. E. 1932. Note sur le boudinage. *Bull. Soc. geol. Fr.* **2**, 477–491.

Williams, P. F. 1985. Multiply deformed terrains—problems of correlation. *J. Struct. Geol.* **7**, 269–280.